Combining Brain Recording Technologies: Using Brain Surfaces

Armin Fuchs, Center for Complex Systems & Brain Sciences, Florida Atlantic University, Boca Raton, FL, USA

1 Introduction

The surfaces of the human cortex like the boundary between the grey and white matter or the pial surface, which separates the grey matter from the cerebral spinal fluid, are strongly folded. The surface areas can be estimated from structural MRI scans and turn out to be 1994cm^2 for the pial surface and 1741cm^2 for the grey-white matter boundary for the subject shown here. A comparison to the surface areas of spheres that contain the same volume (452cm^2 and 290cm^2 for the pial and grey-white matter surface, respectively) shows that major parts of the cortical surfaces are located inside the fissures. The actual shape of these surfaces is of particular interest because due to the columnar organisation of the cortex, the direction of the primary currents is perpendicular to them. Here we show how this knowledge can be used as a constraint for a beamformer in order to estimate local activations inside the brain during a certain task on a time scale at the order of milliseconds.

2 Parameterization of Cortical Surfaces

The work of Dale, Sereno, Fischl and their coworkers provided a powerful software package, known as Freesurfer, to the scientific community [1], [2], [3]. Among other things Freesurfer allows to create tessellated cortical surfaces and to inflate them to various stages for visualization purposes by reducing local curvature, a process that eventually leads to a mapping of these surfaces onto a sphere. This transformation is unique and invertible, i.e. every point on the cortical surfaces corresponds to a single point on the sphere and vice versa. Such a one to one mapping is possible because the spherical and the cortical surfaces are both singly connected and therefore topologically equivalent. As shown in [3], [4] this isomorphism allows for a parameterisation of the cortical surfaces in terms of a spherical coordinate system where each point is defined in terms of two angles, latitude ψ and longitude φ and each pair (ψ,φ) on the sphere corresponds to a location in 3d-space described by its cartesian coordinates (x,y,z).

A grey-scale representation for the z-coordinates of the grey-white matter boundary as functions of ψ and φ is shown in Fig.1 (left) with the values of z increasing from dark to the brighter shades. Plotted in black are the contour lines of a certain constant value of the z-coordinate, which represents the parameterisation in (ψ,φ) of the grey-white matter boundary in an axial slice. The conversion from the spherical representation back to 3d-space is shown in Fig. 1 (right), which also depicts the vectors perpendicular to this surface corresponding to the directions of the primary currents. With this procedure we have a quasi-continuous representation of the cortical surfaces and can sample and tessellate them at whatever accuracy needed.

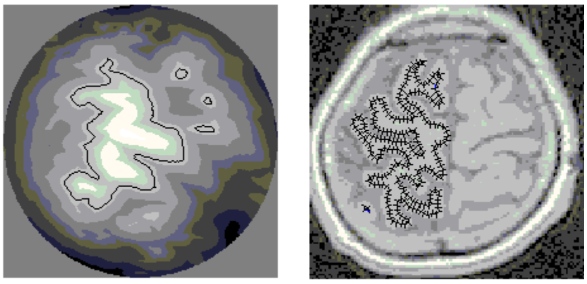

Fig. 1: see text

3 Beamformers

Beamforming is a technique that comes in different flavours [5], [6], [7] and allows to calculate a filter such that an array of electrodes or SQuID sensors becomes most sensitive to a current at a certain location and a certain direction inside a volume. This is achieved by minimizing the power from all other locations and orientations. The EEG or MEG signals that are measured by an array of electrodes or sensors can be represented in form of a vector $\boldsymbol{X}(t)$ whose components correspond to the individual sensors. The signal that originates from a current source at $\boldsymbol{\Theta}$ can then be written in the form $S_{\Theta}(t)=\boldsymbol{H}_{\Theta}\boldsymbol{X}(t)$, where $\boldsymbol{\Theta}=\boldsymbol{\Theta}(x,y,z,\psi,\varphi)$, has to be a 5-dimensional quantity in order to represent both location and direction of the current. The idea now is to minimize the power originating from $\boldsymbol{\Theta}$ over a certain time span, while keeping the contribution from $\boldsymbol{\Theta}$ itself constant. Mathematically, this leads to a minimization problem under constraints of the form

$$S_{\theta}^{2}=\frac{1}{T}\int_{0}^{T}\left\{\boldsymbol{H}_{\theta}\cdot\boldsymbol{X}(t)\right\}^{2}dt\overset{!}{=}Min \qquad (1)$$

with the constraint $\boldsymbol{H}_{\theta}\cdot\boldsymbol{G}_{\theta}=1$, where $\boldsymbol{G}_{\Theta}$ is the forward solution, i.e. the pattern that would be measured in the array from a current source at $\boldsymbol{\Theta}$. Applying the method of Lagrange parameters (1) can be solved leading to

$$\boldsymbol{H}_{\theta}=\frac{\boldsymbol{C}^{-1}\boldsymbol{G}_{\theta}}{\boldsymbol{G}_{\theta}\cdot\boldsymbol{C}^{-1}\boldsymbol{G}_{\theta}} \quad \text{and} \quad S_{\theta}^{2}=\left[\boldsymbol{G}_{\theta}\cdot\boldsymbol{C}^{-1}\boldsymbol{G}_{\theta}\right]^{-1} \qquad (2)$$

where $\boldsymbol{C}$ is the covariance matrix defined as

$$C_{ij} = \frac{1}{T}\int_0^T X_i(t)\, X_j(t)\, dt\,. \qquad (3)$$

In principle, one can now scan a volume (the brain) and calculate an estimate for the source activity at each $\boldsymbol{\Theta}$.

However, if the signal dynamics is low-dimensional, for instance after averaging or with only a few sources active, the covariance matrix does not have an inverse. It is still possible to solve the problem defined by (1) by expanding the beamformer $\boldsymbol{H_\Theta}$ and the forward solution $\boldsymbol{G_\Theta}$ into the eigenvectors $\boldsymbol{v}^{(k)}$ of the covariance matrix $\boldsymbol{C}$.

$$\boldsymbol{H_\theta} = \sum_{k=1}^{M} h_k \boldsymbol{v}^{(k)} \quad \text{and} \quad \boldsymbol{G_\theta} = \sum_{k=1}^{M} g_k \boldsymbol{v}^{(k)} \qquad (4)$$

After straightforward calculations the beamformer coefficients h_k and the source power are found as

$$h_k = \frac{g_k}{\lambda_k}\left\{\sum_{l=1}^{M}\frac{g_l^2}{\lambda_l}\right\}^{-1} \quad \text{and} \quad S_{\boldsymbol{\theta}}^2 = \left\{\sum_{l=1}^{M}\frac{g_l^2}{\lambda_l}\right\}^{-1} \qquad (5)$$

The source power calculated from (2) or (5) cannot be used to directly compare activity strengths obtained from different $\boldsymbol{\Theta}$s, because due to the constraint $\boldsymbol{H_\theta} \cdot \boldsymbol{G_\theta} = 1$ the gain of the beamformer depends on the location and orientation of the source. The power, therefore, has to be normalized by a gain factor, which can be found by calculating the sensitivity of the sensor array to uncorrelated noise from that source. The noise power is given by

$$N_{\boldsymbol{\theta}}^2 = \left[\boldsymbol{G_\theta} \cdot \mu \boldsymbol{\Sigma}^{-1} \boldsymbol{G_\theta}\right]^{-1} \quad \text{or} \quad N_{\boldsymbol{\theta}}^2 = \left\{\sum_{l=1}^{M}\frac{\mu g_l^2}{\sigma_l}\right\}^{-1} \qquad (6)$$

according to (2) or (5), respectively. Here $\boldsymbol{\Sigma}$ is a diagonal matrix representing the noise which can estimated from experimental data, σ_l are the eigenvalues of $\boldsymbol{\Sigma}$, and the parameter μ allows for controlling the sensitivity of the beamformer. Increasing μ from 1 leads to an increase in the signal to noise ratio with the tradeoff that the spatial resolution decreases, i.e. the pattern gets more blurred and less focused. The power adjusted by the gain of the beamformer is given by the ratio $S_{\boldsymbol{\theta}}^2 / N_{\boldsymbol{\theta}}^2$.

4 Local Dynamics from a Beamformer with Strong Anatomical Constraints

The above considerations are applicable to most of the beamforming approaches found in the literature. The main differences are in the way constraints are used. In principle, one could search the 5-dimensional space given by $\boldsymbol{\Theta}$, and algorithms have been proposed to estimate location and direction of a current source that way [7]. SAM [6] restricts the direction of sources to the plane tangential to the surface the sensors are located on, or to the best fitting sphere for this surface, which is particularly useful for MEG as this technology is most sensitive to tangentially oriented sources. This constraint reduces the dimension of the problem because only one angle has to be varied and the largest power found is taken as the activity at that location. Here we will go much further and constrain the locations to points on the grey-white matter boundary and the directions to be the normal vector to the surface at these points as proposed in [1] and also used in [8]. Figure 2 (left) shows activation in left sensori-motor cortex recorded using fMRI during an experiment where a subject was moving the right index finger at a constant rate paced by a metronome. Figure 2 (right) shows the vectors inside the activated area that are located on the grey-white matter boundary and oriented prependicular to this surface. The line thickness indicates the activity found by fMRI for this location, suggesting that the strongest activation takes place inside the walls anterior and posterior to the central sulcus (as expected).

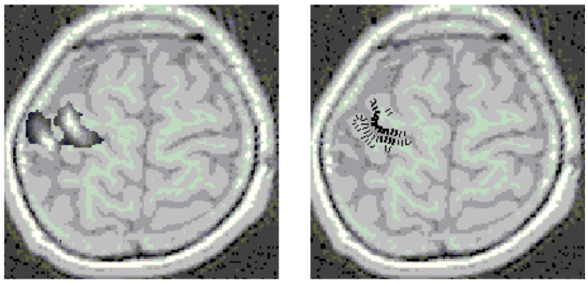

Fig. 2: see text

Figure 3 (top row) shows a blowup of the region around the central sulcus, with normal vectors plotted on the posterior (left in figure) and anterior (right in figure) side. The distance between the vectors on a given side is 2mm measured along the grey-white matter boundary. The beamformer was used to obtain an estimate for the timecourse of the activity at these sites. MEG data was recorded from the same subject under similar experimental conditions and coregistered to the structural and functional MRI datasets as well as the grey-white matter boundary. Then the beamformer coefficients h_k were calculated according to (5) for the different sites and timeseries $S^2_{\boldsymbol{\Theta}}(t)$ for each location were determined by applying the beamformer to the dataset $S^2_{\boldsymbol{\Theta}}(t)=\{\boldsymbol{H_\Theta}\cdot\boldsymbol{X}(t)\}^2$. Results for the posterior and anterior regions of the central sulcus are show in the left and right collumns of the bottom part in Fig. 3, respectively. Here going left to right along the sulcus corresponds to top to bottom in the collumns. A vertical line indicates the time point of maximum finger flexion. The length of each timeseries is 480ms. Plotted as a dotted line is a squared timeseries from a single channel as a reference. From bottom to top the activation shifts from a timepoint prior to peak flexion to a time point after peak flexion in an almost wave like fashion. This corresponds to activity traveling from right to left along the central sulcus as time evolves.

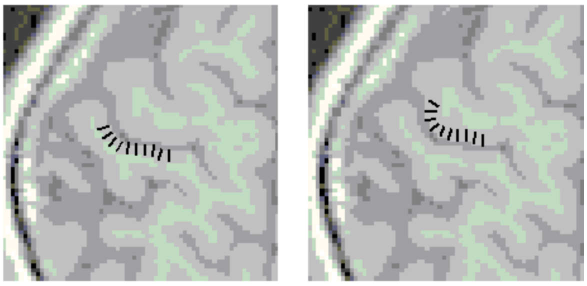

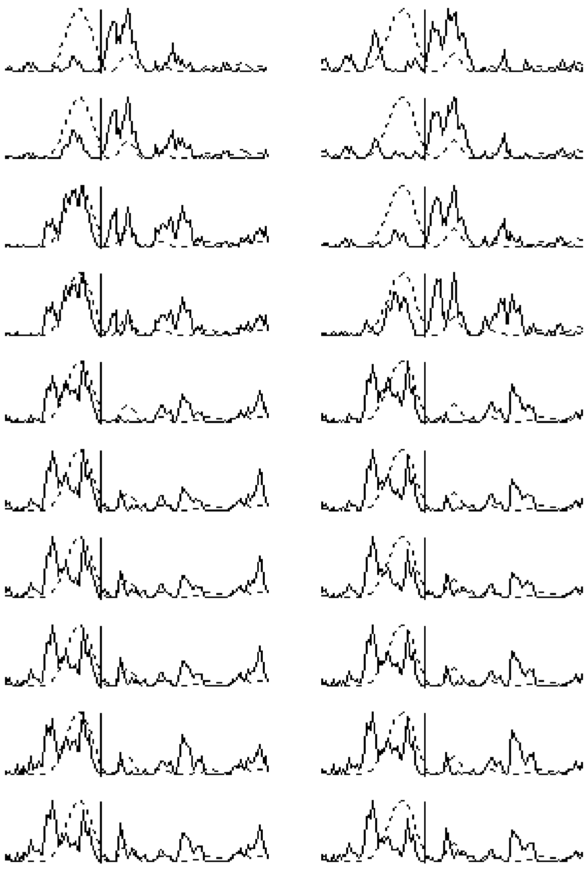

Fig. 3: see text

5 Conclusions

The example shown here is only a first small step in the direction of combining different imaging techniques but nevertheless demonstrates the potential of what kind of insight can be gained by doing so. Reconstruction of the grey-white matter boundary led us to well defined and physiologically relevant constraints for a beamforming algorithm that then allowed us to find the time course of activity in a region of interest identified by functional MRI. A further step would be to include EEG data from the same subject recorded under the same task conditions as it could serve as an independent test for the reliability of the activation sequence found here from MEG recordings. Finally, with the approach presented here it may be possible to find connections between cortical areas by calculating coherences not between the signals from different electrodes or sensors but between different locations on the cortical surfaces.

Work supported by NINDS (grant NS39845), NIMH (grant MH42900) and the Human Frontier Science Program.

6 Literature

[1] Dale A.M, Sereno M.I.: ‘Improved Location of Cortical Activity by Combining EEG and MEG with MRI Cortical Surface Reconstruction: A Linear Approach, *Journal of Cognitive Neuroscience* **5/2:** 162-176 (1993)

[2] Dale A.M., Fischl B., Sereno M.I: ‘Cortical Surface-Based Analysis I: Segmentation and Surface Reconstruction’, *NeuroImage* **9:** 179-194 (1999)

[3] Fischl B., Sereno M.I., Dale A.M.: ‘Cortical Surface-Based Analysis II: Inflation, Flattening, and a Surface-Based Coordinate System’, *NeuroImage* **9:** 195-207 (1999)

[4] Fischl B., Sereno M.I., Tootell R.B.H., Dale A.M.: ‘High-Resolution Intersubject Averaging and a Coordinate System for the Cortical Surface’*, Human Brain Mapping* **8:** 272-284 (1999)

[5] Sekihara K.: ‘Generalized Wiener Estimation of Three-Dimensional Current Distribution from Biomagnetic Measurements’, *IEEE Trans. Biomed. Eng.* **43/3**: 281-291 (1996)

[6] Robinson S.E., Vrba J.: ‘Functional neuroimaging by synthetic aperture magnetometry (SAM)’, in: *Recent Advances in Biomagnetism,* T. Yoshimito, M.Kotani, S. Kuriki, H. Karibe, N. Nakasato, eds., pp. 302-305, Tohoku University Press, Sendai (1999)

[7] Sekihara K., Srikatan S., Nagarajan S.S., Poeppel D., Marantz A., Miyashita Y.: ‘Reconstructing Spatio-Temporal Activities of Neural Sources Using an MEG Vector Beamformer Technique’, *IEEE Trans. Biomed. Eng.* **48/7**: 760-771 (2001)

[8] Fuchs A., Kelso J.A.S.: ‘Combing nonivasive imaging technologies to enhance the spatial and temporal resolution and understanding of brain activity’, *Society for Neuroscience Abstracts* 932.3 (2001)